


Cite this: *Catal. Sci. Technol.*, 2021, **11**, 4406

## A mechanistic investigation of the Suzuki polycondensation reaction using MS/MS methods†

Michelle Y. C. Ting, Lars P. E. Yunker, Ian C. Chagunda,  Katherine Hatlelid, Meghan Vieweg and J. Scott McIndoe \*

Understanding catalytic reactions is inherently difficult because not only is the catalyst the least abundant component in the mixture, but it also takes many different forms as the reaction proceeds. Precatalyst is converted into active catalyst, short-lived intermediates, resting states, and decomposition products. Polymerization catalysis is harder yet to study, because as the polymer grows the identities of these species change with every turnover as monomers are added to the chain. Modern mass spectrometric methods have proved to be up to the challenge, with multiple reaction monitoring (MRM) in conjunction with pressurized sample infusion (PSI) used to continuously probe all stages of the Suzuki polycondensation (SPC) reaction. Initiation, propagation, and termination steps were tracked in real time, as well as the side products from undesirable aryl-phosphine scrambling. The outstanding sensitivity and low signal-to-noise of the approach has real promise with respect to the depth with which this reaction and others like it can be studied.

Received 27th April 2021,  
Accepted 27th May 2021

DOI: 10.1039/d1cy00743b

rsc.li/catalysis

### Introduction

The Suzuki polycondensation reaction (SPC)<sup>1,2</sup> employs palladium catalysts to produce conjugated polymers from difunctional monomers. Interest in the reaction is high thanks to the importance of these polymers to organic light emitting diode (OLED) display technologies.<sup>3,4</sup> It largely employs the same catalysts and conditions as the Suzuki–Miyaura (SM) cross-coupling reaction.<sup>5–8</sup> The SM reaction is a well known palladium-catalysed cross-coupling reaction of organoboron compounds with organic halides.<sup>9</sup> The high yields, reliability, and stereo- and regioselectivity make it one of the most widely used C–C bond forming reactions, with its discovery by Professor Akira Suzuki jointly earning the 2010 Nobel Prize in Chemistry.<sup>9,10</sup> It proceeds in a cycle of three main steps as shown in Scheme 1.<sup>10</sup> The first step is the oxidative addition of an organic halide to a Pd(0) catalyst producing a Pd(II) intermediate. This is followed by the base-mediated transmetalation of the organoboron coupling partner to the Pd(II) intermediate, and finally the reductive elimination of the coupled product and regeneration of the Pd(0) catalyst.<sup>10</sup>

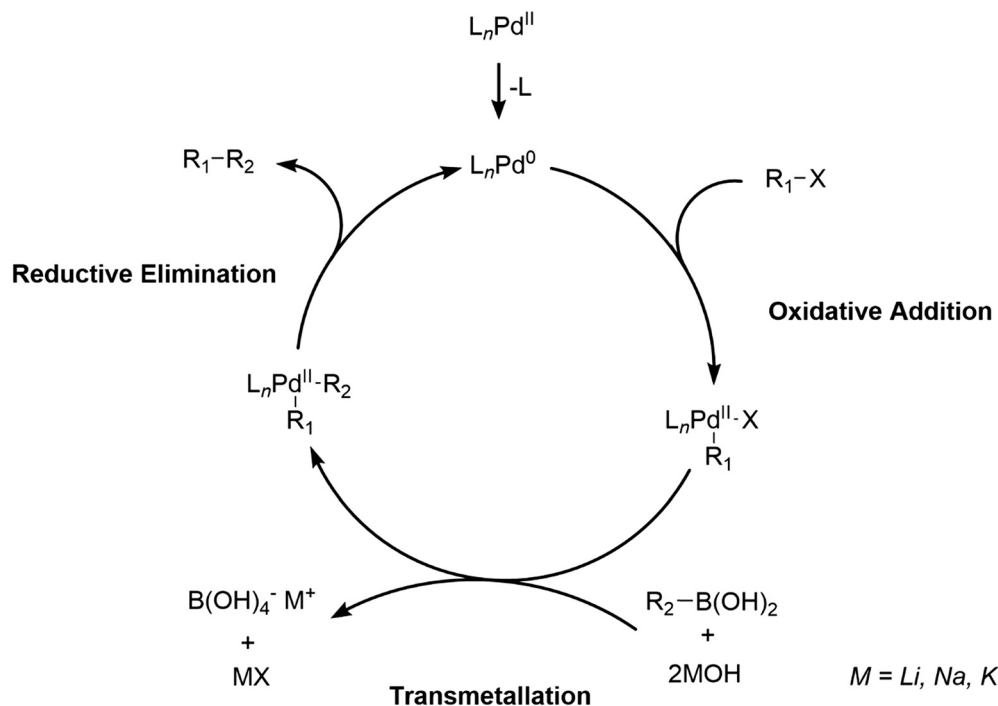
The SPC proceeds through a similar catalytic cycle as the Suzuki–Miyaura reaction, in a polymer-forming process where difunctional aryl monomers connect to form repeating aromatic units.<sup>11</sup> It can be conducted with AB-type monomers, *i.e.* an aryl halide and an aryl boronic acid (or ester) on the same monomer unit, or with AA and BB-type monomers *i.e.* X-aryl-X and (HO)<sub>2</sub>B-aryl-B(OH)<sub>2</sub>.<sup>12–15</sup> With AB-type monomers, the polyarylenes obtained have repeat units of only one kind, while the AA and BB-type monomers can result in both homopolymers or polyarylenes with two kinds of alternating units.<sup>10,11</sup>

Mechanistic interest in the reaction stems from the importance of side reactions becoming magnified by their effect on polymer chain length and identity of end groups. Methods for analyzing the molecular weight distribution of the SPC are well-developed, as they are amenable to all the tools of the polymer chemist.<sup>16</sup> But following the reaction on a molecular level is challenging, because the growing polymer chain repeatedly interacts with the metal catalyst, making the identity of the intermediates and resting states in the reaction change with every turnover.<sup>17</sup> As such, an unusually powerful tool is required for studying the SPC.

Mass spectrometry is fast and extremely sensitive but studying the SPC poses special challenges: no two products or intermediates have the same molecular weight, and so whatever ion intensity one starts with at the beginning of the reaction gets dispersed across many new ions over the course of the reaction. As such, we expected that the normal approach of using conventional full-scan monitoring of the reaction was

Department of Chemistry, University of Victoria, PO Box 1700 STN CSC, Victoria, BC V8W 2Y2, Canada. E-mail: mcindoe@uvic.ca; Fax: +1 (250) 721 7147; Tel: +1 (250) 721 7181

† Electronic supplementary information (ESI) available. See DOI: 10.1039/d1cy00743b



**Scheme 1** Suzuki-Miyaura cross-coupling catalytic cycle.

likely to have limited power to track all the species present, and planned to apply more sophisticated MS/MS methods as necessary. Triple quadrupole mass spectrometers use two quadrupole mass analyzers (MS1 and MS2) separated by a collision cell in which collision-induced dissociation (CID) can break ions into characteristic fragments. These instruments can perform in a variety of modes laid out in Fig. 1.

ESI-MS is a well-established technique for mechanistic studies of organometallic catalytic processes.<sup>18–25</sup> We have previously used real-time mass spectrometric methods to study the Suzuki-Miyaura cross-coupling (SMC) reaction and various other transformations.<sup>26–32</sup> Our standard method of real-time reaction analysis involves transporting a solution from the reaction flask to an electrospray ionization (ESI) mass spectrometer using pressurized sample infusion (PSI).<sup>33,34</sup> ESI-MS provides powerful real-time information, but the technique can observe only ions, not neutrals, so the entities of interest need to carry a charge (inherent, or appended synthetically in a location that does not affect the chemistry under investigation).<sup>35</sup> Our strategy was to start the investigation of the SPC reaction using a charge-tagged aryl iodide [*p*-IC<sub>6</sub>H<sub>4</sub>(CH<sub>2</sub>)PPh<sub>3</sub>]<sup>+</sup>[PF<sub>6</sub>]<sup>−</sup> (**1**<sub>0</sub>) to which we added the Pd(PPh<sub>3</sub>)<sub>4</sub> catalyst. The aryl iodide oxidatively adds to palladium(0) readily, to install the charged tag at one of the termini of the planned polyphenylene oligomers. Addition of a difunctional monomer in the form of *p*-IC<sub>6</sub>H<sub>4</sub>B(OH)<sub>2</sub> would add a  $-(C_6H_4)-$  unit to the oligomer through a transmetallation step, followed by reductive elimination of a new charge-tagged aryl iodide. With each turnover, the new aryl iodide can then oxidatively add to Pd(0) to begin a new cycle, after which the reaction could be terminated *via*

addition of a monofunctional boronic acid, C<sub>6</sub>H<sub>4</sub>B(OH)<sub>2</sub> or *p*-MeOC<sub>6</sub>H<sub>4</sub>B(OH)<sub>2</sub>. The elaborated cycle is shown in Scheme 2. The numbering scheme employed gives all aryl iodide species of the type [Ph<sub>3</sub>PCH<sub>2</sub>C<sub>6</sub>H<sub>4</sub>(C<sub>6</sub>H<sub>4</sub>)<sub>*n*</sub>I]<sup>+</sup> the label **1**<sub>*n*</sub> (where *n* = the number of aryl rings inserted). Similarly, palladium-containing intermediates of the form [(PPh<sub>3</sub>)<sub>2</sub>Pd{(C<sub>6</sub>H<sub>4</sub>)<sub>*n*</sub>C<sub>6</sub>H<sub>4</sub>CH<sub>2</sub>PPh<sub>3</sub>}I]<sup>+</sup> are labelled **2**<sub>*n*</sub>, and **2**<sub>*n*</sub>' for the oxidative addition and transmetallation intermediates respectively. The product oligomers [Ph<sub>3</sub>PCH<sub>2</sub>-C<sub>6</sub>H<sub>4</sub>(C<sub>6</sub>H<sub>4</sub>)<sub>*n*</sub>(C<sub>6</sub>H<sub>5</sub>)]<sup>+</sup> and [Ph<sub>3</sub>PCH<sub>2</sub>C<sub>6</sub>H<sub>4</sub>(C<sub>6</sub>H<sub>4</sub>)<sub>*n*</sub>(C<sub>6</sub>H<sub>4</sub>OMe)]<sup>+</sup> are labelled **3**<sub>*n*</sub> and **4**<sub>*n*</sub> respectively corresponding to the addition of either of the two monofunctional boronic acid capping agents. Note that the Scheme shows only the charged oligomers; following reductive elimination, the oligomer will compete with *p*-IC<sub>6</sub>H<sub>4</sub>B(OH)<sub>2</sub> for oxidative addition to Pd(0). The resulting neutral oligomers are themselves competent as transmetallation partners, so they can still end up with a charged terminus. It is clear that the kinetics of this reaction are likely to be very complicated, even in the absence of any competing side-reactions.

## Results and discussion

To get a sense of the reaction and the type of MS experiments that would be necessary to provide meaningful analyses, we probed the reaction using a variety of different modes.

### Full scan mode

The simplest mode uses a single quadrupole to scan the *m/z* range of interest to generate a mass spectrum of all ions being produced in the source, while the other quadrupole and

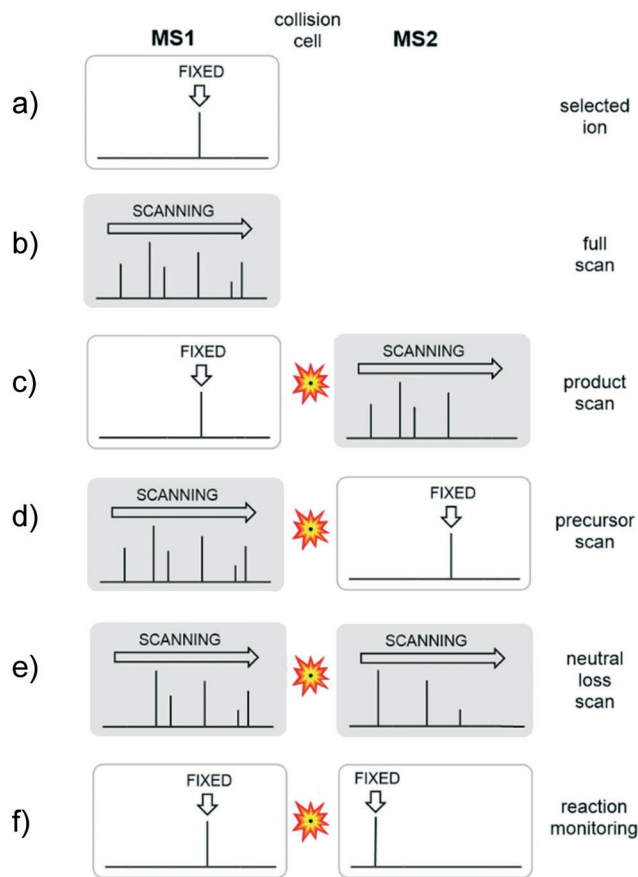


**Fig. 1** (a) One or many ions may be selected using a single quadrupole and their abundance monitored over time; (b) the entire mass-to-charge range of interested can be repetitively scanned in a full-scan mode; (c) an ion may be selected in MS1, fragmented in the collision cell, and the resulting product ions scanned in MS2; (d) MS1 may be set up to scan while MS2 is fixed, which allows only ions with a common fragment to arrive at the detector; (e) MS1 and MS2 are both scanned, with MS2 offset by a fixed value, which allows only ions with a common neutral loss to arrive at the detector; (f) MS1 is fixed at a value of a particular precursor ion, and MS2 is fixed at a value of a particular product ion, so only ions that have a specific  $m/z$  and a specific product ion  $m/z$  arrive at the detector. If this experiment cycles between multiple ions, this process is called multiple reaction monitoring (MRM).

collision cell simply pass all ions through. This is known as full scan mode (Fig. 1b). Applying the full scan mode to the SPC, we used conditions analogous to those we previously employed to examine the Suzuki–Miyaura cross-coupling reaction (methanol solvent, Pd(PPh<sub>3</sub>)<sub>4</sub> catalyst, K<sub>3</sub>PO<sub>4</sub> base, charge-tagged aryl iodide),<sup>31</sup> but instead of using a simple boronic acid as a cross-coupling partner, we used an AB-type monomer, *p*-IC<sub>6</sub>H<sub>4</sub>B(OH)<sub>2</sub>. We tracked the reaction using PSI-ESI-MS using the conditions described in the Experimental section.

All traces were normalized to the total ion current (TIC) and presented in chronogram form in Fig. 2. The numbering scheme employed corresponds to the different catalytic species observed as described in Scheme 2. A stable signal for **1**<sub>0</sub>, the charge-tagged aryl iodide, was established and the Pd(PPh<sub>3</sub>)<sub>4</sub> precatalyst added to the solution at 2 minutes causing a rapid decrease in the intensity of **1**<sub>0</sub>, and an

increase in intensity of **2**<sub>0</sub>. The half-life of this reaction was faster than the time it takes for the solution to move from the reaction vessel to the mass spectrometer, *i.e.*  $t_{1/2} < 20$  s. When the AB monomer substrate was added at 20 minutes, a decrease in intensity of **2**<sub>0</sub> was observed and species corresponding to **1**<sub>1–6</sub> and **2**<sub>2–4</sub> appeared sequentially, indicating that reaction turnover had occurred. Little change to the speciation occurred beyond 40 minutes, so a capping agent, C<sub>6</sub>H<sub>5</sub>B(OH)<sub>2</sub>, was added at 44 minutes and **3**<sub>0–4</sub> were observed. SPC reactions are typically left for hours or overnight to react.<sup>36–39</sup> Under the conditions used, the reaction appears to have turned over 0–6 times in the 80 minute observation period. A summation of all mass spectra collected over these 80 minutes of reaction time is shown in Table S1 of the ESI.†

The full scan mode chronogram shows the general flow of reactants, intermediates, and products through this cycle as expected, though with considerable limitations. The high signal noise makes the traces barely intelligible, with some of the signals lost in the baseline and requiring multiplication by a factor of 20 to be observed at all. Some species also appeared to be present before it was physically possible for them to be there as the corresponding reagent was not injected into the reaction mixture until later. For example, **2**<sub>1–2</sub> showed a low intensity before the AB monomer was added, and **3**<sub>1</sub> is very prominent, appearing at the beginning of the reaction at 0 minutes. Such behavior was deemed to be due to the presence of conflating species and contaminants with the same  $m/z$  as the catalytic species of interest. This would also point to side reactions occurring at the palladium center, with phosphine ligand scrambling a known side reaction that may result in speciation with overlapping  $m/z$ .<sup>40–43</sup> However, the limitations of the full scan mode for overlapping  $m/z$  did not provide adequate information to unambiguously identify these species. There are also several unassigned mass peaks in the mass spectrum, which are likely to be cesium carbonate aggregates, trace impurities from previous analyses, species formed from methanolysis and contaminants from the septa when reagents were injected into the reaction mixture.<sup>44</sup> Nonetheless, it was clear that the chemistry could be studied despite the fact the intermediates and products changed in  $m/z$  with every turnover, though the methodology needed improvement. For that we attempted to narrow the scope of species analyzed using the selected ion recording (SIR) mode.

### Selected ion recording (SIR)

With the known target species in hand, we could start applying different methods to get more reliable, selective, and sensitive chronograms of the catalytic reaction. The first method we tried was selected ion recording (SIR), an approach that can be employed by any scanning MS instrument. Instead of scanning the entire mass range, only the ions of interest are targeted. The most intense peak of a particular isotope envelope, or the most intense peak unaffected by overlap with another species,

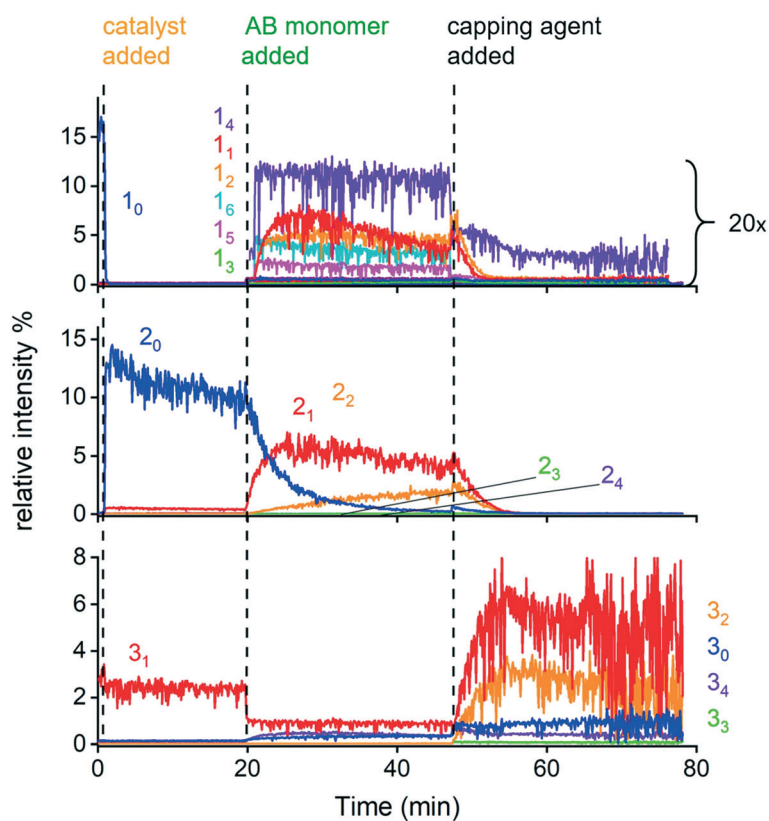
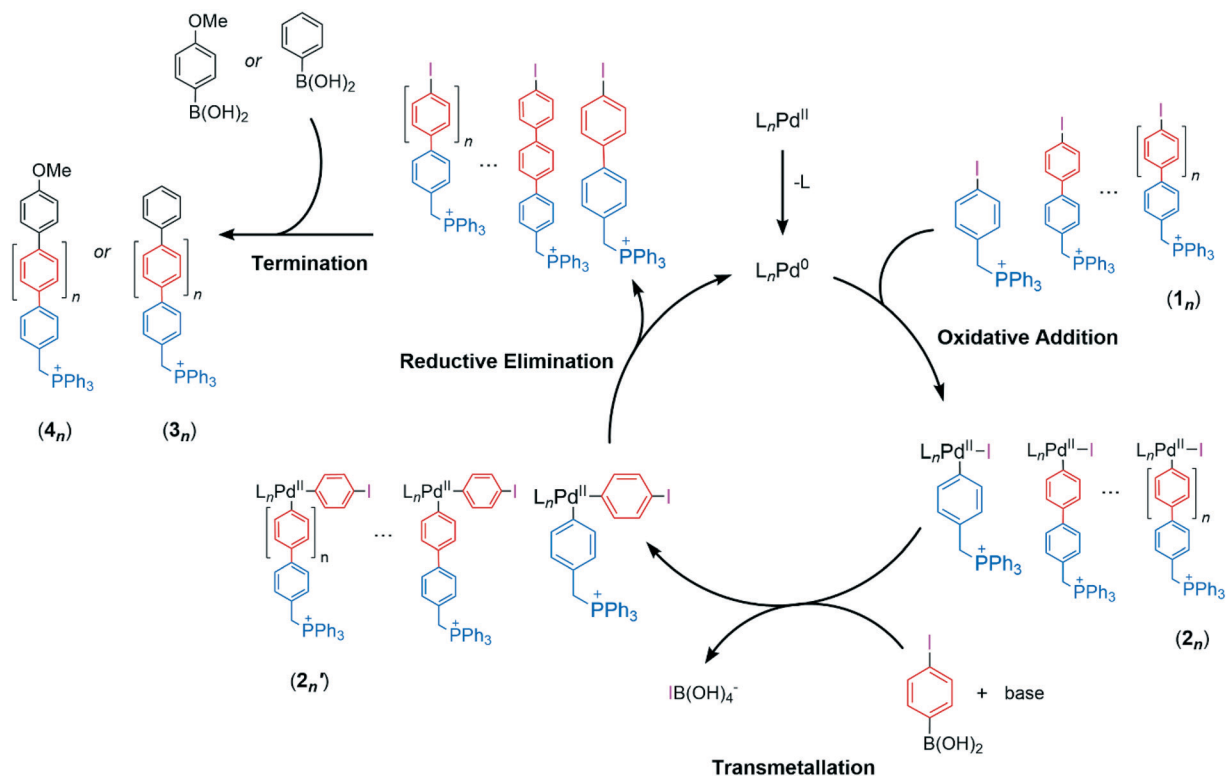


**Fig. 2** The normalized PSI-ESI-MS full scan chronogram of the SPC. Aryl iodide species are label as  $1_n$ , intermediates as  $2_n$ , and capped oligomer products as  $3_n$  ( $n = 1-6$ ). The  $\text{Pd}(\text{PPh}_3)_4$  precatalyst, AB monomer *p*-(OH)<sub>2</sub>BC<sub>6</sub>H<sub>4</sub>I and the end-capping agent C<sub>6</sub>H<sub>5</sub>B(OH)<sub>2</sub> was added to the reaction solution at 2 minutes, 20 minutes, and 44 minutes as indicated with dotted lines.

can be selected, and the amount of time each species is dwelled upon can be customized. Also, the mass spectrum of SIR experiment does not show the isotopic pattern, just the selected mass peak(s) and their intensity, further simplifying the spectrum produced.

For this experiment, the  $m/z$  ratio of each catalytic species was calculated and input into the mass spectrometer. The dwell time of the Pd-containing species was set to be longer than that of the aryl iodide and oligomeric product species to increase the S:N ratio. The amount of AB monomer was adjusted to 6 equivalents instead of 12 since species with  $n > 5$  were not observed. All other reaction conditions and mass spectrometer settings remained the same in order to compare results with the full scan chronogram. The normalized chronogram of each set of species is shown in Fig. 3 following the same sequence of substrate addition as with the full scan chronogram.

The SIR chronogram showed significant improvements in the traces of all species and appeared cleaner and more intelligible. Low intensity species observed in a full scan chronogram were amplified in an SIR chronogram by adjusting the dwell time upwards, with additional baseline multiplication by a factor of seven. Upon AB monomer addition,  $2_{1-4}$  showed a significant increase in relative intensity and decrease when the capping agent was added to the reaction mixture. Why the palladium-containing species

$2_n$  behave better than the aryl iodides  $1_n$  in this respect may be due to their relative  $m/z$  values – low mass ions are more likely to experience adventitious overlap than higher mass ions. Aside from the  $2_n$  intermediates, we were also able to observe the capped oligomers  $3_{0-4}$  when the capping agent was added at 57 minutes, which in contrast showed very low intensity in the full scan chronogram. However, their behavior is still clearly non-physical. The capped oligomers  $3_n$  appeared long before the capping reagent itself was added, and similar problematic behavior was seen for the  $2_n$  species appearing prior to AB monomer addition. This presents the challenge of how to differentiate when a trace is coming from background noise, or overlapping species, or from part of the catalytic cycle.

### Neutral loss mode

To help solve the problem of coincidental overlap, we turned to MS/MS methods. A product ion scan is the most common MS/MS experiment. A precursor ion is selected in MS1 and undergoes collision-induced dissociation to produce a product ion and a neutral fragment. The product ion is then detected in MS2 (Fig. 1c). Product ion scans were performed on  $1_{0-4}$ ,  $2_{0-1}$ , and  $3_{0-4}$  which revealed that all ions under study decompose in the gas phase under CID conditions to lose triphenylphosphine (PPh<sub>3</sub>; see ESI† Fig. S1–S6). We optimised the collision voltage

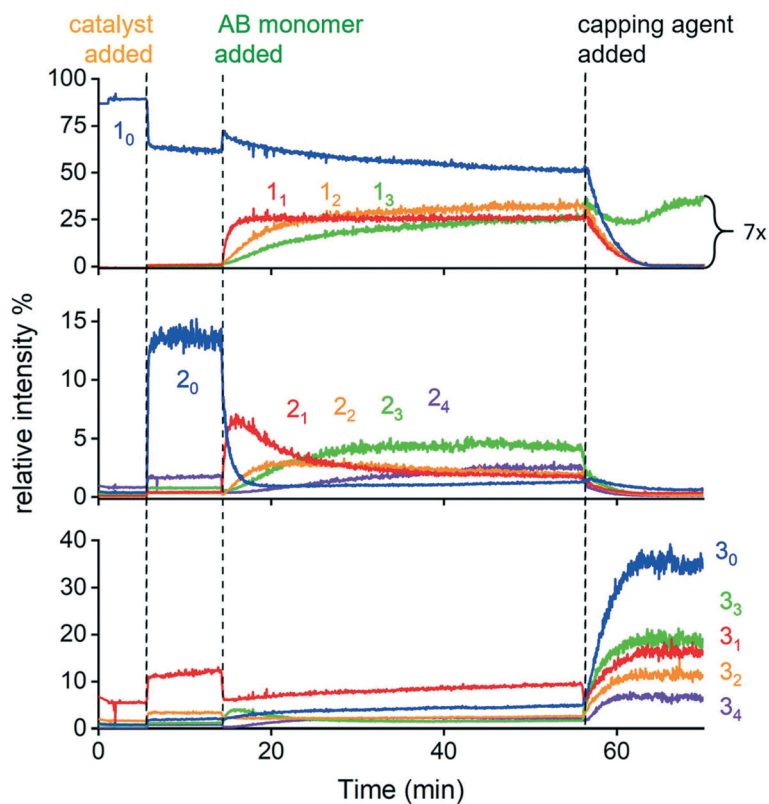


Fig. 3 The normalized ESI-MS SIR chronogram of the SPC showing the relative intensity of aryl iodide species label as  $1_n$ , intermediates as  $2_n$ , and the end-capped oligomer products as  $3_n$  ( $n = 0-4$ ). The Pd(PPh<sub>3</sub>)<sub>4</sub> precatalyst, AB monomer *p*-(OH)<sub>2</sub>BC<sub>6</sub>H<sub>4</sub>I, and the end-capping agent C<sub>6</sub>H<sub>5</sub>-B(OH)<sub>2</sub> was added to the reaction solution at 5 minutes, 14 minutes, and 57 minutes respectively (indicated in dotted lines).

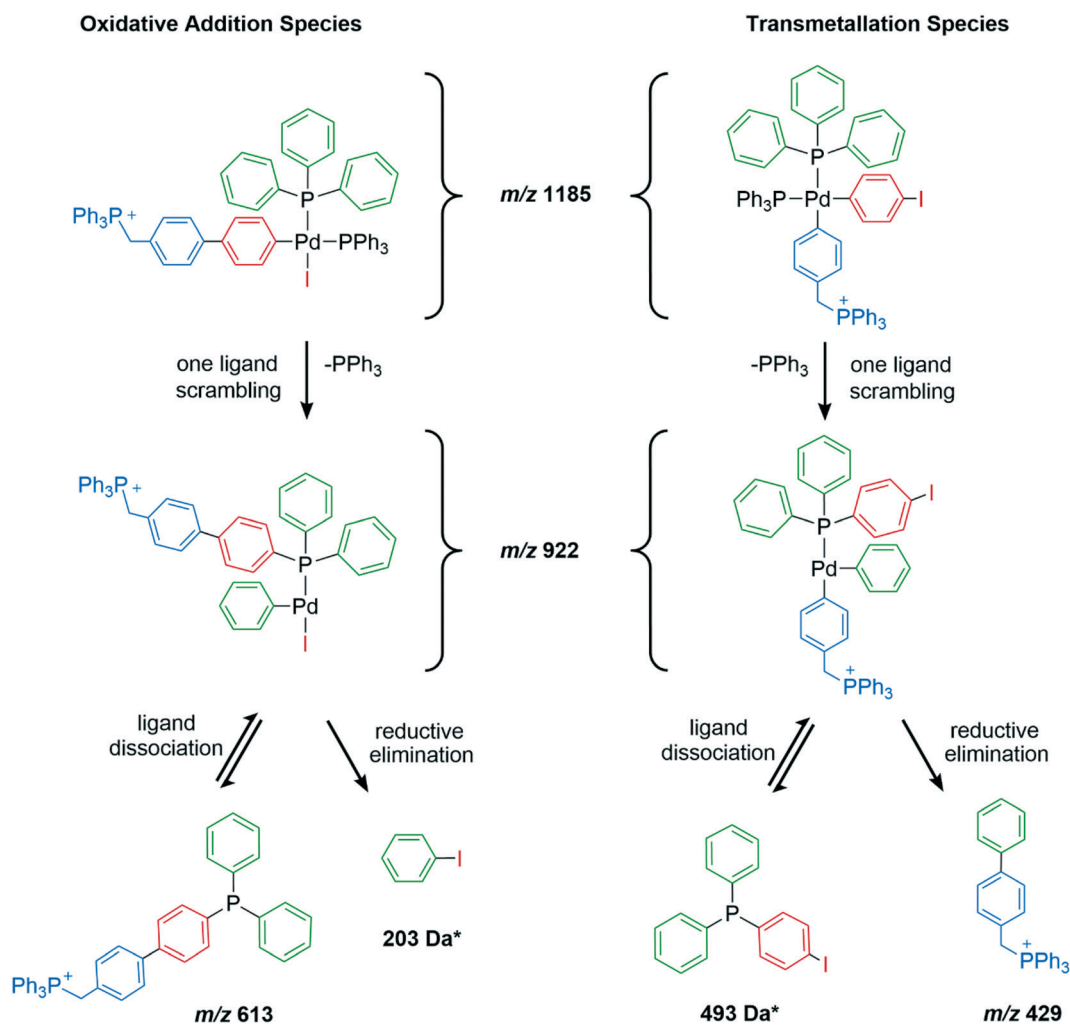


for maximum abundance of the product ion in each case, with  $2_n$  ions needing 15–20 V lower than that required for  $1_n$  and  $3_n$  (30–35 V).  $\text{PPh}_3$  (an L-type ligand) is readily lost from palladium through a simple ligand dissociation, hence the lower voltage required compared to decomposition of the triphenylphosphonium tag. L-type ligands tend to dissociate first because they are stable as free entities, while X-type ligands take more energy for homolytic dissociation due to the requirement of radical formation.<sup>29,31,45,46</sup>

The results of the MS/MS analysis on  $2_n$  species helped explain the peculiar behavior of the capped oligomers  $3_{0-4}$  in the full scan and SIR chromatogram. We used phenylboronic acid,  $\text{C}_6\text{H}_4\text{B}(\text{OH})_2$  as the capping agent for the SPC and found that the predicted  $m/z$  ratio of the capped oligomers would have the same  $m/z$  ratio as the phosphine scrambling products. Each tandem mass spectrum of  $2_{1-3}$  showed low abundance signals at  $m/z$  429, 505, 581 that are assigned as aryl phosphine scrambling products through the transmetallation species pathway,  $\text{Ar}^+(\text{C}_6\text{H}_4)\text{H}$ ,  $\text{Ar}^+(\text{C}_6\text{H}_4)_2\text{H}$  and  $\text{Ar}^+(\text{C}_6\text{H}_4)_3\text{H}$ . An example of possible phosphine scrambling pathway for the  $2_1$  intermediate is shown

in Scheme 3. For the oxidative addition species, a  $\text{PPh}_3$  fragment is first lost then the phosphonium-charged aryl group can swap with a phenyl group on the remaining Pd-bound  $\text{PPh}_3$ . This aryl interchanged product may further reductively eliminate to form an iodobenzene product (203 Da) or dissociate as the phosphine ( $m/z$  613). The transmetallation species would have a similar pathway as the oxidative addition species but will lead to different product formation as illustrated. Since ESI-MS can only detect charged speciation, iodobenzene and  $\text{Pd}(\text{PPh}_2\text{C}_6\text{H}_5\text{I})$  cannot be observed.

It would therefore be possible to observe species with  $m/z$  ratios matching  $3_{0-4}$  prior to the addition of the capping agent in the full scan and SIR chromatograms. Their appearance indicated that there is a substantial amount of phosphine scrambling going on, and that we should not consider the behaviour of  $3_{0-4}$  as background noise or adventitious overlapping species. We addressed this complication of overlapping  $m/z$  due to phosphine scrambling by switching to a different capping agent, methoxyphenylboronic acid  $p\text{-MeOC}_6\text{H}_4\text{B}(\text{OH})_2$ , with the new



**Scheme 3** Comparison of the proposed aryl-phosphine scrambling mechanism of the oxidative addition species and the transmetallation species considered for  $2_1$ .

capped products  $[\text{Ph}_3\text{PCH}_2\text{C}_6\text{H}_4(\text{C}_6\text{H}_4)_n\text{OMe}]^+$  ( $4_n$ ) having different masses from the phosphine scrambling products (+30 Da, see ESI† Table S1). We further modified the product ion scan mode to using the neutral scan mode.

Because all species decompose by the same fragmentation pathway,  $\text{PPh}_3$  elimination, setting up a neutral loss scan was straightforward. In a neutral loss scan, both MS1 and MS2 are scanning together but MS2 scans with a mass offset equivalent to the neutral loss of interest. All ions are allowed to pass through MS1 to undergo the CID process, but only ions that lose a common neutral fragment after the CID process are detected in MS2 (Fig. 1e). Moreover, the neutral loss scan enables two or more functions set up with different collision energy to interweave in the same scan to obtain ions that give out different fragmentation pattern at different collision energy. The data is collected into one single raw file with two (or more) functions with two mass spectra and two chronograms and each mass spectrum displays ion peak(s) that are detected at the specific collision energy. This scan mode is especially beneficial to study the SPC as it increases the signal-to-noise ratio by excluding ions that do not lose a  $\text{PPh}_3$  fragment (262 Da), but bear the same  $m/z$  ratio as the  $1_n$ ,  $2_n$ , and  $4_n$  species of interests. Since the product ion scan experiments revealed that each series did not exhibit the same fragmentation at the same collision energy, it was possible to set up one experiment with multiple functions of

neutral loss scans to detect ions of all series of interest at their optimal collision energy.

The normalized chronogram of the neutral loss scan is shown in Fig. 4 and all reaction conditions remained the same as with full scan and SIR experiments. A multiplier was not necessary, as each trace showed an observable relative intensity. The aryl iodides  $1_{0-4}$  and Pd-containing species  $2_{0-4}$  exhibited a sequential increase in intensity much like the full scan and the SIR chronogram, and a relatively stable sequential increase and decrease in intensity during catalyst addition at 12 minutes and AB monomer addition at 18 minutes. The methoxyphenylboronic acid capping agent was added at 36 minutes, with both  $1_{0-4}$  and  $2_{0-4}$  showing gradual decreases in their relative intensity and  $4_{0-4}$  showing increases in their relative intensity. The neutral loss scan chronogram showed a further reduction of chemical noise in comparison to the full scan and SIR chronograms. It has also eliminated what appears to be a significant problem with the  $1_n$  species, which in SIR mode maintain significant intensity even after the addition of the precatalyst  $\text{Pd}(\text{PPh}_3)_4$ . The  $1_0$  species ought to be reactive towards oxidative addition, and the neutral loss scan confirms this, as it dropped intensity rapidly after addition of the precatalyst.

Unlike SIR, which increases signal but does nothing about noise and overlap ion peaks, the neutral loss scans are useful for reducing noise and overlapping species but do not help

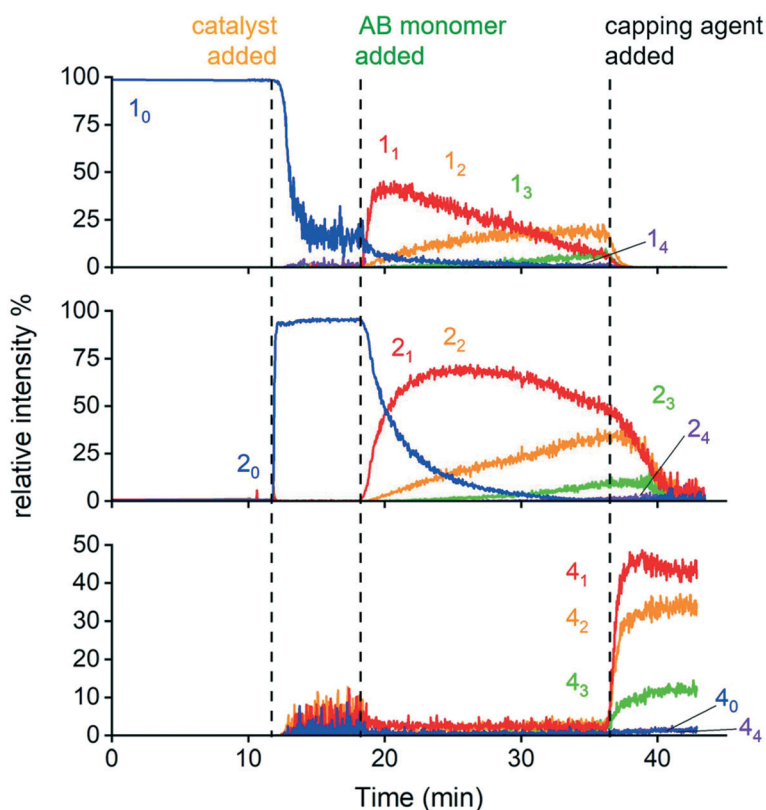


Fig. 4 The normalized PSI-ESI-MS neutral loss scan chronogram of the SPC showing the relative intensity of aryl iodide species label as  $1_n$ , intermediates as  $2_n$ , and new capped oligomer products as  $4_n$  ( $n = 0-4$ ). The precatalyst  $\text{Pd}(\text{PPh}_3)_4$ , AB monomer  $p\text{-(HO)}_2\text{BC}_6\text{H}_4\text{I}$  and the end-capping agent  $\text{MeOC}_6\text{H}_4\text{B(OH)}_2$  was added at 12 minutes, 18 minutes, and 36 minutes indicated with dotted lines.

in increasing the signal intensity. The signal intensity increases emerge by ensuring the scanning instrument spends its time focused only on the peaks of interest. The experimental results of the neutral loss scan are satisfactory in terms of sensitivity and selectivity of the SPC monitoring, but triple quadrupole mass spectrometers still have another mode to exploit: multiple reaction monitoring (MRM).

### Multiple reaction monitoring

MRM is a rapid, highly sensitive and selective screening method used for monitoring one or multiple specific ion transition(s).<sup>47–51</sup> The collision energy is optimized to produce a diagnostic charged fragment of that ion (already established from the product ion scan experiments). Many MRM experiments can be compiled together into one experiment to measure many specific ions in a complex mixture. It is crucial to obtain precursor ion and product ion information along with ionization and fragmentation parameters prior to an MRM experiment. MRM methods can then be easily set up by inputting the precursor and product ion  $m/z$ , the collision voltage, and the dwell time and span of the peak. This mode provided the best and most chemically sensible data of all the approaches. Similar to an SIR experiment, MRM does not generate a mass spectrum with

isotopic patterns but a single peak at the pre-selected  $m/z$  ratio, typically chosen to be the most intense signal in the isotopomer envelope, with the relative intensity of this peak shown in the extracted ion chromatogram.

The MRM chromatogram of the SPC reaction is shown in Fig. 5. At time 0,  $1_0$  can be observed and was consumed at the addition of the precatalyst, Pd(PPh<sub>3</sub>)<sub>4</sub> at 8 minutes and accompanied by the appearance of  $2_0$ . When the AB monomer was added at 12 minutes, a decrease in intensity of  $2_0$  was observed and species corresponding to  $1_{1-4}$  and  $2_{1-4}$  appeared sequentially, indicating that reaction turnover had occurred. The capping agent, MeOC<sub>6</sub>H<sub>4</sub>B(OH)<sub>2</sub>, was added at 38 minutes and all the  $4_{0-4}$  products were produced rapidly. It was also noted that the relative intensity of  $4_{3,4}$  were shown to decrease right after its appearance in this experiment. Overall, the result of the MRM appears to be very clean, species of interest no longer appeared at the beginning of the chromatogram, meaning that species (apart from  $1_0$ ) that appear at 0 min in the full scan and SIR results were likely to be S:N artefacts or contaminants.

What does the MRM data tell us about the reaction? First, it needs to be appreciated that the species we see do not represent the complete story. After reductive elimination of each new biaryl compound, the catalyst has several available options: it can oxidatively add to the charge-tagged polyaryl

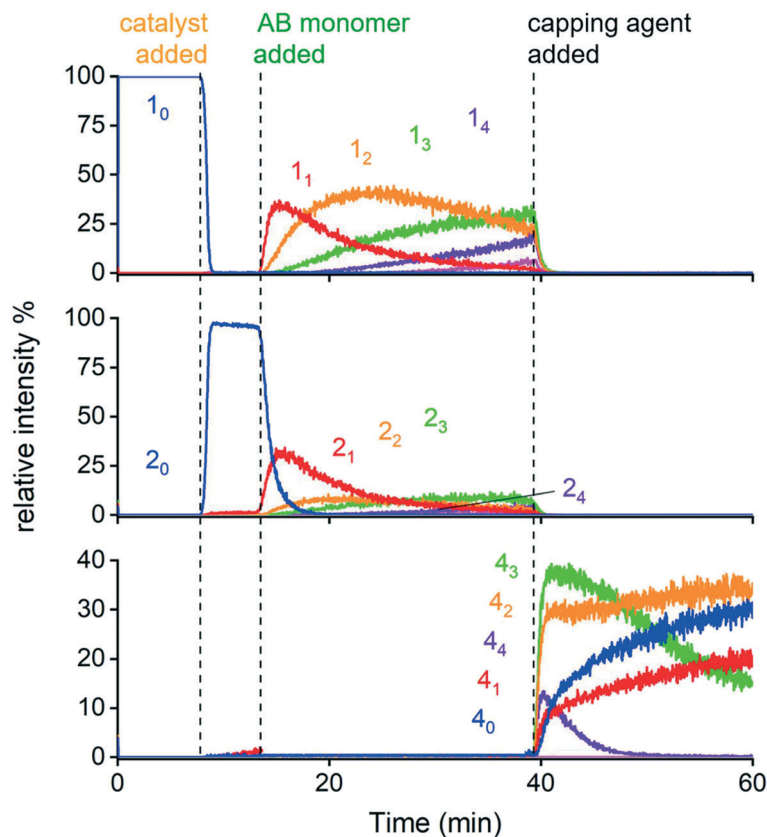
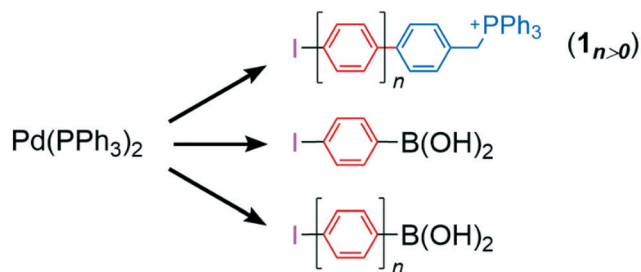


Fig. 5 The normalized PSI-ESI-MS MRM chromatogram of the SPC showing the relative intensity of aryl iodide species label as  $1_n$ , intermediates as  $2_n$ , and capped oligomer products as  $4_n$  ( $n = 0-4$ ). The precatalyst Pd(PPh<sub>3</sub>)<sub>4</sub>, AB monomer  $p$ -(OH)<sub>2</sub>BC<sub>6</sub>H<sub>4</sub>I and the end-capping agent MeOC<sub>6</sub>H<sub>4</sub>-B(OH)<sub>2</sub> was added at 8 minutes, 12 minutes, and 38 minutes indicated in dotted lines.





**Scheme 4** Possible partners for oxidative addition following reaction turnover.

iodide  $1_{n>0}$ , the difunctional AB monomer  $\text{IC}_6\text{H}_4\text{B}(\text{OH})_2$ , or an untagged difunctional polyaryl iodide,  $\text{I}(\text{C}_6\text{H}_4)_n\text{B}(\text{OH})_2$ , all of which have an available reactive Ar-I bond. Only one of these is charged, and so a certain proportion of the reaction mixture goes undetected (Scheme 4).

It is also possible that the transmetalation step can be between a tagged species and a difunctional polyaryl species of the type  $(\text{HO})_2\text{B}(\text{C}_6\text{H}_4)_n\text{I}$ , in which case the oligomer will grow by multiple monomer units in a single turnover.

A further question remains concerning the  $2_n$  species. There is some ambiguity in the composition of these species (except for  $2_0$ ), although we can be certain they are of the general formula  $[(\text{Ph}_3\text{P})_2\text{Pd}\{(\text{C}_6\text{H}_4)_n\text{CH}_2\text{PPh}_3\}\text{I}]^+$ . There are four options: the two sets of *cis* and *trans* isomers for each of  $[(\text{Ph}_3\text{P})_2\text{Pd}\{(\text{C}_6\text{H}_4)_n\text{CH}_2\text{PPh}_3\}\text{I}]^+$ , where the ligands are aryl and iodide, and  $[(\text{Ph}_3\text{P})_2\text{Pd}\{(\text{C}_6\text{H}_4)_n\text{CH}_2\text{PPh}_3\}(\text{C}_6\text{H}_4)_n\text{I}]^+$ , where the ligands are both aryl. MS/MS examination can assist with untangling the ambiguity, since bis(aryl) palladium species are prone to reductive elimination of a biaryl species,<sup>52,53</sup> whereas an aryl palladium iodide is not. Product ion scans of each Pd-containing species showed little evidence for reductive elimination of the biaryl species  $\text{Ar}^+(\text{C}_6\text{H}_4)_n\text{I}$  as product ions (a small amount of  $m/z$  555,  $\text{Ar}^+(\text{C}_6\text{H}_4)_2\text{I}$ , was seen in the product ion spectrum of  $[(\text{Ph}_3\text{P})_2\text{Pd}\{(\text{C}_6\text{H}_4)_2\text{CH}_2\text{PPh}_3\}\text{I}]^+$ , but only after  $\text{PPh}_3$  loss), suggesting that the partitioning of this intermediate is strongly biased towards aryl/iodide complexes of the type  $[(\text{Ph}_3\text{P})_2\text{Pd}\{(\text{C}_6\text{H}_4)_n\text{CH}_2\text{PPh}_3\}\text{I}]^+$ . We were not able to discern whether the aryl/iodide complexes are *cis* or *trans*. Instead of reductive elimination, we saw  $\text{PPh}_3$  dissociation as the dominant pathway for gas-phase unimolecular decomposition. Following that, other pathways are unlocked that reveal the propensity of these systems for aryl-phosphine scrambling (see Scheme 3 and Fig. S1–S4†).<sup>40–43,54,55</sup> Evidence for this process included the appearance of fragment ions such as  $[\text{Ph}_3\text{PCH}_2(\text{C}_6\text{H}_4)_n\text{PPh}_2]^+$  and  $[\text{PPh}_4]^+$ . Aryl phosphine scrambling is a notorious side reaction that is problematic for the SPC because it reduces the polyaryl chain length.<sup>56</sup> The earlier observation that the  $3_n$  species appeared right after AB monomer addition observed in the full scan and SIR chronogram is strong solution-phase evidence that phosphine scrambling is taking place, and the MS/MS experiments confirm that these transformations can be duplicated in the gas phase.

The final step of the reaction was to cap the oligomers using a monofunctional boronic acid, either  $\text{PhB}(\text{OH})_2$ , or in later reactions,  $p\text{-MeOC}_6\text{H}_4\text{B}(\text{OH})_2$ . Both reacted rapidly with all of the oligomeric species in solution to generate the capped oligomers of the form  $[\text{Ph}_3\text{PCH}_2(\text{C}_6\text{H}_4)_n(\text{C}_6\text{H}_5)]^+$  and  $[\text{Ph}_3\text{PCH}_2(\text{C}_6\text{H}_4)_n\text{OMe}]^+$ . The behaviour of  $4_3$  and  $4_4$  were unusual as their intensity first increased as expected, then unexpectedly decreased, in an especially pronounced way for  $4_4$ . The most obvious reason for this observation is that these extended polyaryl species have limited solubility, and that we are monitoring a precipitation event for  $4_3$  and (particularly)  $4_4$  rather than any sort of special reactivity. Note that under such conditions, the loss of charged species from solution will have an effect on the remaining species due to the normalization applied, so the apparent growth in the  $4_{0-2}$  species is a function of the precipitation of the other ions rather than a continuing reaction producing more capped oligomer (see the abrupt disappearance of  $1_{0-4}$  and  $2_{0-4}$ ).

The formation of the oligomer product series  $4_n$  studied in each method were shown to have a dramatic increase as soon as the addition of capping agent terminated the ongoing catalytic cycle, suggesting that SPC is a step-growth polymerization. This observation is consistent with the SMC mechanism and the SPC literature as it would be impossible to observe the catalytic species ( $1_{2-4}$  and  $2_{2-4}$ ) at the same time had the reaction proceeded in a chain-growth fashion.

## Experimental

Reagents were purchased from Sigma-Aldrich and were used without further purification. Methanol (HPLC grade) was distilled from calcium hydride before every use. Gases were purchased from Airgas (Calgary, Canada) and used without further purification. All experiments and reagents were performed under nitrogen atmosphere using standard Schlenk and glovebox techniques. All mass spectra were collected by a Waters Acquity Triple Quadrupole Mass spectrometer equipped with a Z-Spray pneumatically assisted electrospray ionization source in the positive ion mode.

Synthesis of the charged tag  $[\text{Ph}_3\text{PCH}_2\text{C}_6\text{H}_4\text{I}]^+[\text{PF}_6]^-$  ( $1_0$ ) was as previously reported.<sup>57</sup> Stock solutions of  $1_0$ , 4-iodophenylboronic acid, 4-methoxyphenylboronic acid, and phenylboronic acid were prepared in MeOH at concentrations of 0.5, 3.0, 1.0, and 1.0  $\text{mmol L}^{-1}$  respectively. Tetrakis(triphenylphosphine) palladium(0) (11.5 mg) was prepared in 4 mL of THF for each experiment. All solutions were kept in a glovebox until ready for use.

All reactions were monitored using PSI-ESI-MS under the following conditions. Methanol (20 mL), stirrer bar, and  $\text{K}_3\text{PO}_4$  base (2 mg, 9  $\mu\text{mol}$ ) was added to the Schlenk flask at a bath temperature of 40 °C. The charged aryl iodide,  $[\text{Ph}_3\text{PCH}_2\text{C}_6\text{H}_4\text{I}]^+[\text{PF}_6]^-$  ( $1_0$ , 0.4 mL of the 0.5  $\text{mmol L}^{-1}$  stock solution, 0.2  $\mu\text{mol}$ ) was added to the flask by syringe through a septum. After a short period (~10 minutes), a solution of the  $\text{Pd}(\text{PPh}_3)_4$  precatalyst (11.5 mg, 10  $\mu\text{mol}$  in 4 mL of THF) was added until all of  $1_0$  was consumed. After about 10 minutes, the AB

monomer,  $\text{IC}_6\text{H}_4\text{B}(\text{OH})_2$  (0.8 ml of the  $3.0 \text{ mmol L}^{-1}$  stock solution,  $2.4 \mu\text{mol}$ ) was added by syringe. The reaction was allowed to proceed for about 40 minutes before the capping reagent,  $\text{C}_6\text{H}_5\text{B}(\text{OH})_2$  or  $\text{MeOC}_6\text{H}_4\text{B}(\text{OH})_2$  ( $1.0 \text{ mL}$  of the  $1.0 \text{ mmol L}^{-1}$  stock solution,  $1.0 \mu\text{mol}$ ) was added by syringe. Data collection continued for a further 20 minutes.

## Conclusions

Real-time monitoring and MS/MS methods proved capable of analysing the Suzuki polycondensation reaction, and despite the complexity of the system, key features of the reaction could be determined. The reaction was performed using aryl iodides, so the oxidative addition step of the reaction was rapid, and the reaction was shown by product ion MS/MS (as well as isotope pattern and  $m/z$  characterization) to rest at the intermediate with aryl and iodide ligands,  $(\text{Ph}_3\text{P})_2\text{Pd}(\text{Ar}^+)$ . I. The reaction turned over several times in the space of 30 minutes, and generated oligomers containing up to four monomer units. These oligomers could be efficiently terminated by use of a monofunctional boronic acid. Capping resulted in the higher monomers decaying in intensity, an observation attributed to a lack of solubility as chain length increases. A complicating feature of the reaction was aryl-phosphine ligand scrambling, a phenomenon observed here both in solution phase and in the gas phase under collision-induced dissociation.

The reaction initially consisted of a single charged species, the charge-tagged aryl iodide,  $\text{Ar}^+\text{I}$ . As the reaction proceeded, new species emerged as the tag was oxidatively added to the palladium(0) catalyst, and coupled to monomer units as the reaction proceeded through transmetallation and reductive elimination steps, and back through the cycle again with an increased  $m/z$  value. As such, the charge was distributed across increasingly many different masses, each of which needed to be measured constantly. Such a task was made easier by the application of different scanning modes in the triple quadrupole mass spectrometer employed. Monitoring of specific ions of interest increased signal, as the instrument dwells only on ions of interest, but this approach does not alleviate complexities of accidental overlap with unrelated species. The neutral loss mode solved this problem, finding only species that exhibited a neutral loss of  $\text{PPh}_3$  (a feature of both the charge-tagged species and of the  $\text{PPh}_3$  ligands on palladium), but distorted the relative abundances of the various species as the extent of fragmentation varied for each ion. Multiple reaction monitoring proved the most powerful, providing excellent signal-to-noise ratios at the cost of a highly customized experimental setup.

Advice for practitioners wanting to apply these methods to their own systems: it is best to first get a sense of the overall reaction using the full-scan mode. While the dynamics are likely to be noisy, a good idea of the relative rates of reaction will be established and combination of all scans will provide a mass spectrum whose baseline can be mined for even minor species. Some knowledge of the fragmentation

behavior of the ions of interest will allow analysis *via* neutral loss scans and will help inform the setup of the MRM mode when the best quality data is desired.

## Conflicts of interest

There are no conflicts to declare.

## Acknowledgements

J. S. M. thanks the NSERC Discovery program for operational funding and NSERC RTI and the University of Victoria for infrastructural support.

## References

- 1 M. Rehahn, A.-D. Schlüter, G. Wegner and W. J. Feast, *Polymer*, 1989, **30**, 1054–1059.
- 2 J. Sakamoto, M. Rehahn, G. Wegner and A. D. Schlüter, *Macromol. Rapid Commun.*, 2009, **30**, 653–687.
- 3 G. Li, Y. Zhao, J. Li, J. Cao, J. Zhu, X. W. Sun and Q. Zhang, *J. Org. Chem.*, 2015, **80**(1), 196–203.
- 4 C. Baskar, Y.-H. Lai and S. Valiyaveetil, *Macromolecules*, 2001, **34**(18), 6255–6260.
- 5 N. Miyaoura, K. Yamada and A. Suzuki, *Tetrahedron Lett.*, 1979, **20**, 3437–3440.
- 6 N. Miyaoura and A. Suzuki, *Chem. Rev.*, 1995, **95**, 2457–2483.
- 7 A. Suzuki, *Angew. Chem., Int. Ed.*, 2011, **50**, 6722–6737.
- 8 L.-C. Campeau and N. Hazari, *Organometallics*, 2019, **38**, 3–35.
- 9 A. Suzuki, *Chem. Commun.*, 2005, 4759–4763.
- 10 A. Krishna, A. V. Lunchev and A. C. Grimsdale, Suzuki Polycondensation, in *Synthetic Methods for Conjugated Polymers and Carbon Materials*, ed. M. Leclerc and J.-F. Morin, Wiley-VCH, Weinheim, Germany, 2017, pp. 59–95.
- 11 J. Sakamoto, M. Rehahn and D. Schlüter, in *Design and Synthesis of Conjugated Polymers*, John Wiley & Sons Ltd, 2010, pp. 45–90.
- 12 A.-D. Schlüter, C. J. Hawker and J. Sakamoto, *Synthesis of polymers: new structures and methods*, Wiley-VCH, 2012.
- 13 M. E. Rogers, T. E. Long and S. R. Turner, in *Synthetic Methods in Step-Growth Polymers*, John Wiley & Sons, Inc., Hoboken, NJ, USA, 2003, pp. 1–16.
- 14 R.-D. Rusu and A. D. Schlüter, *RSC Adv.*, 2014, **4**, 57026–57034.
- 15 A. D. Schlüter, *J. Polym. Sci., Part A: Polym. Chem.*, 2001, **39**, 1533–1556.
- 16 G. Dhangar, J. L. Serrano, C. Schulzke, K. C. Gunturu and A. R. Kapdi, *ACS Omega*, 2017, **2**(7), 3144–3156.
- 17 P. Chen, *Angew. Chem., Int. Ed.*, 2003, **42**, 2832–2847.
- 18 C. Markert and A. Pfaltz, *Am. Ethnol.*, 2004, **116**, 2552–2554.
- 19 F. di Lena, E. Quintanilla and P. Chen, *Chem. Commun.*, 2005, 5757–5759.
- 20 D. Schröder, *Acc. Chem. Res.*, 2012, **45**, 1521–1532.
- 21 F. Bächle, J. Duschmalé, C. Ebner, A. Pfaltz and H. Wennemers, *Angew. Chem., Int. Ed.*, 2013, **52**, 12619–12623.

- 22 C. Iacobucci, S. Reale, M. Aschi, J. Oomens, G. Berden and F. De Angelis, *Chem. – Eur. J.*, 2018, **24**, 7026–7032.
- 23 A. Ray, T. Bristow, C. Whitmore and J. Mosely, *Mass Spectrom. Rev.*, 2018, **37**, 565–579.
- 24 D. B. Eremin, E. A. Denisova, A. Y. Kostyukovich, J. Martens, G. Berden, J. Oomens, V. N. Khrustalev, V. M. Chernyshev and V. P. Ananikov, *Chem. – Eur. J.*, 2019, **25**, 16564–16572.
- 25 D. Agrawal and D. Schröder, *Organometallics*, 2011, **30**, 32–35.
- 26 K. Vikse, G. N. Khairallah, J. S. McIndoe and R. A. J. O'Hair, *Dalton Trans.*, 2013, **42**, 6440.
- 27 E. Crawford, T. Lohr, E. M. Leitao, S. Kwok and J. S. McIndoe, *Dalton Trans.*, 2009, 9110.
- 28 K. L. Vikse, M. A. Henderson, A. G. Oliver and J. S. McIndoe, *Chem. Commun.*, 2010, **46**, 7412.
- 29 K. L. Vikse and J. S. McIndoe, *Pure Appl. Chem.*, 2015, **87**, 361–377.
- 30 K. Vikse, T. Naka, J. S. McIndoe, M. Besora and F. Maseras, *ChemCatChem*, 2013, **5**, 3604–3609.
- 31 K. L. Vikse, Z. Ahmadi, C. C. Manning, D. A. Harrington and J. S. McIndoe, *Angew. Chem., Int. Ed.*, 2011, **50**, 8304–8306.
- 32 Z. Ahmadi, A. G. Oliver and J. S. McIndoe, *ChemPlusChem*, 2013, **78**, 632–635.
- 33 K. L. Vikse, M. P. Woods and J. S. McIndoe, *Organometallics*, 2010, **29**, 6615–6618.
- 34 K. L. Vikse, Z. Ahmadi, J. Luo, N. van der Wal, K. Daze, N. Taylor and J. S. McIndoe, *Int. J. Mass Spectrom.*, 2012, **323–324**, 8–13.
- 35 J. H. Gross, in *Mass Spectrometry*, Springer International Publishing, Cham, 2017, pp. 721–778.
- 36 R.-D. Rusu and A. D. Schlüter, *RSC Adv.*, 2014, **4**, 57026–57034.
- 37 K. Zhang, R. Tkachov, K. Ditte, N. Kiriy, A. Kiriy and B. Voit, *Macromol. Rapid Commun.*, 2020, **41**, 1900521.
- 38 H. Sugita, Y. Ohta and T. Yokozawa, *J. Polym. Sci.*, 2020, **58**, 1236–1240.
- 39 H. Sugita, M. Nojima, Y. Ohta and T. Yokozawa, *Polym. Chem.*, 2019, **10**, 1182–1185.
- 40 D. K. Morita, J. K. Stille and J. R. Norton, *J. Am. Chem. Soc.*, 1995, **117**, 8576–8581.
- 41 J. Frahn, B. Karakaya, A. Schäfer and A.-D. Schlüter, *Tetrahedron*, 1997, **53**, 15459–15467.
- 42 B. Hohl, L. Bertschi, X. Zhang, A. D. Schlüter and J. Sakamoto, *Macromolecules*, 2012, **45**, 5418–5426.
- 43 D. Agrawal, E.-L. Zins and D. Schröder, *Chem. – Asian J.*, 2010, **5**, 1667–1676.
- 44 E. O. Pentsak, D. B. Eremin, E. G. Gordeev and V. P. Ananikov, *ACS Catal.*, 2019, 3070–3081.
- 45 L. P. E. Yunker, Z. Ahmadi, J. R. Logan, W. Wu, T. Li, A. Martindale, A. G. Oliver and J. S. McIndoe, *Organometallics*, 2018, **37**, 4297–4308.
- 46 W. Henderson and J. S. McIndoe, *Mass Spectrometry of Inorganic, Coordination and Organometallic Compounds*, John Wiley & Sons, Ltd, Chichester, UK, 2005.
- 47 B. Domon and R. Aebersold, *Science*, 2006, **312**, 212–217.
- 48 A. J. Norris, J. P. Whitelegge, K. F. Faull and T. Toyokuni, *Biochemistry*, 2001, **40**, 3774–3779.
- 49 S. A. Carr and L. Anderson, *Clin. Chem.*, 2008, **54**, 1749–1752.
- 50 Y. Wang, W.-Y. Lin, K. Liu, R. J. Lin, M. Selke, H. C. Kolb, N. Zhang, X.-Z. Zhao, M. E. Phelps, C. K. F. Shen, K. F. Faull and H.-R. Tseng, *Lab Chip*, 2009, **9**, 2281.
- 51 D. D. Khanal, Y. Z. Baghdady, B. J. Figard and K. A. Schug, *Rapid Commun. Mass Spectrom.*, 2019, **33**, 821–830.
- 52 K. L. Vikse, M. A. Henderson, A. G. Oliver and J. S. McIndoe, *Chem. Commun.*, 2010, **46**, 7412–7414.
- 53 G. T. Thomas, E. Janusson, H. S. Zijlstra and J. S. McIndoe, *Chem. Commun.*, 2019, **55**, 11727–11730.
- 54 R. Qian, Y.-X. Liao, Y.-L. Guo and H. Guo, *J. Am. Soc. Mass Spectrom.*, 2006, **17**, 1582–1589.
- 55 M. Leclerc and J.-F. Morin, *Synthetic methods for conjugated polymers and carbon materials*, Wiley-VCH, 2017.
- 56 F. E. Goodson, T. I. Wallow and B. M. Novak, *Macromolecules*, 1998, **31**, 2047–2056.
- 57 K. L. Vikse, Z. Ahmadi, C. C. Manning, D. A. Harrington and J. S. McIndoe, *Angew. Chem., Int. Ed.*, 2011, **50**, 8304–8306.